

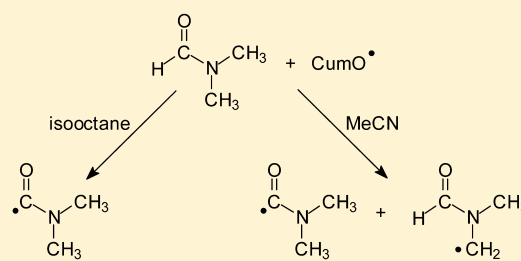
# Kinetic Solvent Effects on the Reactions of the Cumyloxy Radical with Tertiary Amides. Control over the Hydrogen Atom Transfer Reactivity and Selectivity through Solvent Polarity and Hydrogen Bonding

Michela Salamone, Livia Mangiacapra, and Massimo Bietti\*

Dipartimento di Scienze e Tecnologie Chimiche, Università "Tor Vergata", Via della Ricerca Scientifica 1, I-00133 Rome, Italy

**S** Supporting Information

**ABSTRACT:** A laser flash photolysis study on the role of solvent effects on hydrogen atom transfer (HAT) from the C–H bonds of *N,N*-dimethylformamide (DMF), *N,N*-dimethylacetamide (DMA), *N*-formylpyrrolidine (FPRD), and *N*-acetylpyrrolidine (APRD) to the cumyloxy radical (CumO•) was carried out. From large to very large increases in the HAT rate constant ( $k_H$ ) were measured on going from MeOH and TFE to isooctane ( $k_H(\text{isooctane})/k_H(\text{MeOH}) = 5\text{--}12$ ;  $k_H(\text{isooctane})/k_H(\text{TFE}) > 80$ ). This behavior was explained in terms of the increase in the extent of charge separation in the amides determined by polar solvents through solvent–amide dipole–dipole interactions and hydrogen bonding, where the latter interactions appear to play a major role with strong HBD solvents such as TFE. These interactions increase the electron deficiency of the amide C–H bonds, deactivating these bonds toward HAT to an electrophilic radical such as CumO•, indicating that changes in solvent polarity and hydrogen bonding can provide a convenient method for deactivation of the C–H bond of amides toward HAT. With DMF, a solvent-induced change in HAT selectivity was observed, suggesting that solvent effects can be successfully employed to control the reaction selectivity in HAT-based procedures for the functionalization of C–H bonds.



## INTRODUCTION

The study of solvent effects on hydrogen atom transfer (HAT) attracts continuous interest because these reactions are involved in chemical and biological processes of fundamental importance. Relevant examples include the antioxidant ability of radical-scavenging substrates,<sup>1</sup> enzymatic reactions,<sup>2</sup> the oxidative damage to biomolecules,<sup>3</sup> the decomposition of organic compounds in the atmosphere,<sup>4</sup> and procedures for the functionalization of C–H bonds.<sup>5</sup> In these studies, reactive oxygen-centered radicals such as alkoxy radicals have received great attention. These radicals can be conveniently generated by UV photolysis from easily available precursors, are known to undergo hydrogen abstraction from several classes of substrates, and can tolerate a variety of experimental conditions. Accordingly, these features make alkoxy radicals particularly convenient for the study of solvent and medium effects on HAT reactions.<sup>6</sup>

Among the different classes of hydrogen atom donors, phenolic compounds have been thoroughly studied because these substrates represent the most extensive class of radical-scavenging antioxidants.<sup>1,7</sup> Accordingly, a description of the mechanistic details of solvent effects on HAT reactions from the O–H bonds of phenolic substrates to alkoxy radicals (as well as to other radicals) has been provided.<sup>8</sup> In these studies, significant kinetic solvent effects (KSEs) have been observed on HAT reactions from a variety of phenols to two representative tertiary alkoxy radicals such as *tert*-butoxy ((CH<sub>3</sub>)<sub>3</sub>CO•,

*t*BuO•) and cumyloxy (PhC(CH<sub>3</sub>)<sub>2</sub>O•, CumO•), where an up to 3 orders of magnitude increase in  $k_H$  was measured on going from 2-methyl-2-propanol and/or methanol to isooctane, i.e. on decreasing solvent hydrogen bond acceptor (HBA) ability. This behavior was accounted for on the basis of a hydrogen bond interaction between the solvent and the phenolic OH, with HAT that only occurs from the free OH group. Accordingly, in HBA solvents HAT involves the desolvated substrate, thus accounting for the observed KSE, with the magnitude of this effect that reflects the strength of the solvent–substrate hydrogen bond interaction.

In the study of solvent effects on HAT reactions from C–H bonds, our research group has recently studied in detail KSEs on the reactions of CumO• with a series of hydrogen atom donor substrates, highlighting the role played by hydrogen bond interactions.<sup>6,9–11</sup> With hydrocarbon substrates such as cyclohexane<sup>9</sup> and 1,4-cyclohexadiene,<sup>10,11</sup>  $k_H$  values are essentially solvent independent in aprotic solvents. A 3- to 4-fold increase in  $k_H$  has been measured on going from these solvents to a strong hydrogen bond donor (HBD) solvent such as 2,2,2-trifluoroethanol (TFE). As previously described, the transition state for HAT from C–H bonds to oxygen-centered radicals such as hydroxyl and alkoxy displays a certain extent of internal charge separation, with the development of a partial

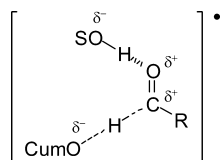
Received: November 24, 2014

Published: December 29, 2014

positive charge on the carbon of the incipient radical and a partial negative charge on the oxygen atom of the abstracting radical.<sup>12</sup> According to this picture, the observed KSEs have been explained in terms of a hydrogen bond interaction between the solvent and the oxygen atom of the radical, interaction that increases in strength on going from the reactants to the transition state, leading, as compared to aprotic solvents, to a larger extent of stabilization of the transition state than of the reactants.

With substrates such as triethylamine (TEA),<sup>11</sup> tetrahydrofuran (THF),<sup>9</sup> propanal (PA), and 2,2-dimethylpropanal (DMPA),<sup>10</sup> characterized by the presence of a HBA site in proximity of the abstractable C–H, an up to 10-fold decrease in  $k_{\text{H}}$  was measured on going from isooctane to MeOH and/or TFE. This behavior was rationalized on the basis of polar contributions to the transition state. HBD solvents can interact with the substrate heteroatom by hydrogen bonding, and such interaction decreases the electron density in proximity of the incipient carbon radical leading, as compared to non-HBD solvents, to a destabilization of the transition state (Scheme 1,

Scheme 1



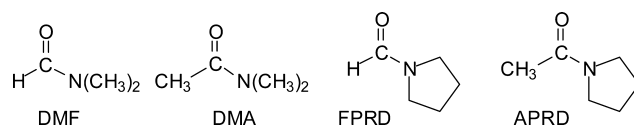
showing the effect of an HBD solvent SOH on the transition state for HAT from the formyl C–H bond of an aldehyde to CumO<sup>•</sup>). In the reactions with TEA and THF it was proposed that also the decrease in the degree of overlap between the  $\alpha$ -C–H bond and the heteroatom lone pair determined by solvent hydrogen bonding plays an important role.<sup>9,11</sup>

Amides are relatively strong hydrogen bond acceptors, displaying HBA abilities that are very similar to those of alkylamines,<sup>13</sup> and this feature suggests, on the basis of the picture outlined above, that sizable KSEs should also be observed in HAT reactions that involve these substrates. To the best of our knowledge, however, no information is presently available on the role played by solvent effects on HAT reactions from amide substrates. Such information would be of great interest because amides are often taken as simple models for the peptide bond, and HAT reactions from amides to alkoxy radicals are currently employed in a large number of procedures for C–H bond functionalization.<sup>15</sup>

Within this framework, in order to expand our recent findings and to provide a more detailed understanding of the role of the solvent on HAT from aliphatic C–H bonds to alkoxy radicals, we have performed a laser flash photolysis study in different solvents (isooctane, benzene, MeCN, 2-methyl-2-butanol (MBOH), MeOH, and TFE) on the reactions of *N,N*-dimethylformamide (DMF), *N,N*-dimethylacetamide (DMA), *N*-formylpyrrolidine (FPRD), and *N*-acetylpyrrolidine (APRD) (Chart 1), with CumO<sup>•</sup>.

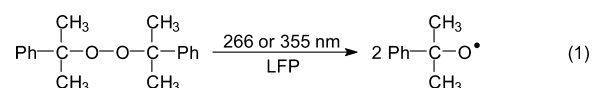
In order to obtain information on the role of solvent effects on the HAT selectivity, the reactions of *N,N*-dimethylformamide-*d*<sub>1</sub> (DMF-*d*<sub>1</sub>), *N,N*-dimethylformamide-*d*<sub>6</sub> (DMF-*d*<sub>6</sub>), and *N,N*-dimethylformamide-*d*<sub>7</sub> (DMF-*d*<sub>7</sub>) with CumO<sup>•</sup> have been investigated in isooctane with comparison to the corresponding reactions studied previously in MeCN solution.<sup>16</sup>

Chart 1



## RESULTS

CumO<sup>•</sup> was generated by laser flash photolysis (LFP) (266 or 355 nm) of argon-saturated dicumyl peroxide solutions, at  $T = 25\text{ }^{\circ}\text{C}$  (eq 1).



It is well-known that in isooctane, benzene, MBOH, and MeCN, CumO<sup>•</sup> is characterized by a visible absorption band at 485 nm,<sup>17</sup> whose position is shifted toward the red in solvents such as MeOH<sup>18</sup> and TFE.<sup>8c,19</sup> With the exclusion of the LFP experiments performed in isooctane and MeOH solution, where competition with HAT from the solvent is observed,<sup>18,20</sup> in all the other solvents the most important decay pathway of CumO<sup>•</sup> is represented by cleavage C–CH<sub>3</sub> ( $\beta$ -scission).<sup>17,20</sup>

The kinetic study of the reactions of the amides displayed in Chart 1 with CumO<sup>•</sup> was carried out by LFP. We have recently shown that in acetonitrile, HAT from DMF and FPRD occurs in competition between the formyl C–H and the C–H bonds of the methyl or methylene groups that are  $\alpha$  to nitrogen, with the former site being the preferred one for DMF.<sup>16</sup> With FPRD, HAT mostly occurs from the pyrrolidine  $\alpha$ -C–H bonds, a behavior that reflects the operation of stereoelectronic effects (i.e., the possibility of achieving optimal orbital overlap between these bonds and the amide  $\pi$ -system).<sup>21</sup> The reactions of CumO<sup>•</sup> with DMA and APRD result in preferential HAT from the *N*-methyl groups and pyrrolidine  $\alpha$ -C–H bonds, with HAT from the acetyl methyl group occurring in both cases as a minor pathway, in agreement with the observation that the former C–H bonds are weaker by at least 5 kcal mol<sup>−1</sup> than the C–H bonds that are adjacent to the carbonyl group.<sup>16,21</sup>

The time-resolved kinetic studies were performed monitoring the decay of the CumO<sup>•</sup> visible band as a function of the concentration of added substrate. When the observed rate constants ( $k_{\text{obs}}$ ) were plotted against substrate concentration, excellent linear relationships were observed and the second-order rate constants for HAT to CumO<sup>•</sup> ( $k_{\text{H}}$ ) were derived from the slopes of these plots. As a representative example, the  $k_{\text{obs}}$  vs [substrate] plots for the reactions of CumO<sup>•</sup> with DMF, DMA, FPRD, and APRD measured in isooctane solution ( $T = 25\text{ }^{\circ}\text{C}$ ) are displayed in Figure 1.

When the reaction of CumO<sup>•</sup> with DMF, DMA, and APRD was studied in TFE solution, a decrease in  $k_{\text{obs}}$  with increasing substrate concentration was instead observed (Figures S1–S3 in the Supporting Information (SI)). In TFE, the unimolecular rate constant for CumO<sup>•</sup> C–CH<sub>3</sub>  $\beta$ -scission ( $k_{\beta}$ ) is significantly higher than in polar aprotic solvents ( $k_{\beta} = 6.1 \times 10^6$  and  $6.3 \times 10^5\text{ s}^{-1}$ , for TFE<sup>19</sup> and MeCN,<sup>20</sup> respectively) and a decrease in  $k_{\beta}$  with increasing added amide by a dilution effect can be reasonably expected. Along this line, the observed behavior clearly indicates that the decrease in  $k_{\text{obs}}$  determined by the effect of added amide on  $k_{\beta}$  is larger than the contribution to  $k_{\text{obs}}$  determined by HAT from the amide to CumO<sup>•</sup>. In order to test this hypothesis, the effect of MeCN on the decay of

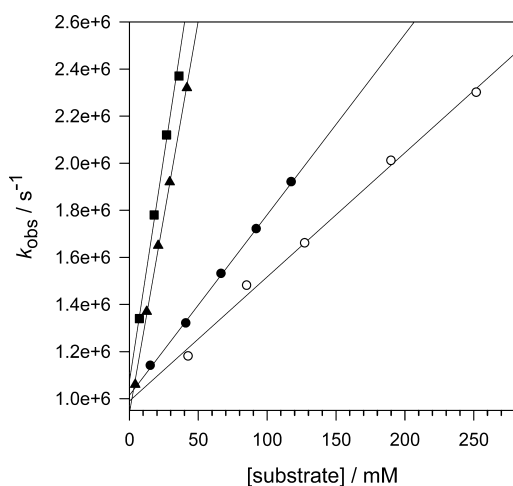


**Figure 1.** Plots of the observed rate constant ( $k_{\text{obs}}$ ) against [substrate] for the reactions of the cumyloxy radical ( $\text{CumO}^\bullet$ ) with *N,N*-dimethylformamide (DMF, black circles), *N,N*-dimethylacetamide (DMA, white circles), *N*-formylpyrrolidine (FPRD, black triangles), and *N*-acetylpyrrolidine (APRD, black squares), measured in argon-saturated isooctane solution at  $T = 25\text{ }^\circ\text{C}$  by following the decay of  $\text{CumO}^\bullet$  at 490 nm. From the linear regression analysis:  $\text{CumO}^\bullet + \text{DMF}$ , intercept =  $1.06 \times 10^6\text{ s}^{-1}$ ,  $k_{\text{H}} = 7.83 \times 10^6\text{ M}^{-1}\text{ s}^{-1}$ ,  $r^2 = 0.9990$ .  $\text{CumO}^\bullet + \text{DMA}$ , intercept =  $9.90 \times 10^5\text{ s}^{-1}$ ,  $k_{\text{H}} = 5.27 \times 10^6\text{ M}^{-1}\text{ s}^{-1}$ ,  $r^2 = 0.9954$ .  $\text{CumO}^\bullet + \text{FPRD}$ , intercept =  $9.39 \times 10^5\text{ s}^{-1}$ ,  $k_{\text{H}} = 3.33 \times 10^7\text{ M}^{-1}\text{ s}^{-1}$ ,  $r^2 = 0.9991$ .  $\text{CumO}^\bullet + \text{APRD}$ , intercept =  $1.07 \times 10^6\text{ s}^{-1}$ ,  $k_{\text{H}} = 3.80 \times 10^7\text{ M}^{-1}\text{ s}^{-1}$ ,  $r^2 = 0.9941$ .

$\text{CumO}^\bullet$  in TFE was investigated, and a decrease in  $k_{\text{obs}}$  with increasing [MeCN] was observed (Figure S4 in the SI). The electron-poor C–H bonds of MeCN are strongly deactivated toward HAT to an electrophilic radical such as  $\text{CumO}^\bullet$  ( $k_{\text{H}} < 10^4\text{ M}^{-1}\text{ s}^{-1}$ )<sup>6,12a,20</sup> so that under these conditions no significant contribution to  $k_{\text{obs}}$  deriving from HAT can be expected, and the observed decrease in  $k_{\text{obs}}$  reflects the decrease in  $k_{\beta}$  determined by MeCN addition. By comparing the dilution effect of MeCN on  $k_{\text{obs}}$  with those observed for DMF, DMA, and APRD, a correction to the measured  $k_{\text{obs}}$  values was applied (see the SI for a description of the procedure) and an upper limit to the  $k_{\text{H}}$  values for reaction of  $\text{CumO}^\bullet$  with the amides in TFE could be obtained as  $k_{\text{H}} < 1 \times 10^4\text{ M}^{-1}\text{ s}^{-1}$  for DMF and DMA and  $k_{\text{H}} < 5 \times 10^5\text{ M}^{-1}\text{ s}^{-1}$  for APRD.

The plots for HAT from DMF, FPRD, DMA, and APRD to  $\text{CumO}^\bullet$  in the different solvents and the plots for HAT from DMF-*d*<sub>1</sub>, DMF-*d*<sub>6</sub>, and DMF-*d*<sub>7</sub> to  $\text{CumO}^\bullet$  in isooctane are displayed in the SI (Figures S6–S10). The  $k_{\text{H}}$  values measured for reaction of  $\text{CumO}^\bullet$  with the four amides in the different solvents are collected in Table 1.

Table 2 displays the  $k_{\text{H}}$  values for reaction of  $\text{CumO}^\bullet$  with DMF, DMF-*d*<sub>1</sub>, DMF-*d*<sub>6</sub>, and DMF-*d*<sub>7</sub> measured in isooctane solution with comparison to the corresponding  $k_{\text{H}}$  values measured previously in MeCN.<sup>16</sup>

## DISCUSSION

The data displayed in Table 1 show that for all four amides the  $k_{\text{H}}$  values for reaction with  $\text{CumO}^\bullet$  decrease by 5–12 times on going from isooctane to MeOH. A much larger decrease in reactivity has been observed in TFE, quantified on the basis of the upper limit to  $k_{\text{H}}$  obtained for reaction of  $\text{CumO}^\bullet$  with DMF, DMA, and APRD, in a >790, >480, and >80-fold decrease in  $k_{\text{H}}$  as compared to isooctane. To the best of our

**Table 1.** Second-Order Rate Constants ( $k_{\text{H}}$ ) for Reaction of the Cumyloxy Radical ( $\text{CumO}^\bullet$ ) with Tertiary Amides, Measured in Different Solvents at  $T = 25\text{ }^\circ\text{C}$ <sup>a</sup>

substrate	solvent	$\lambda_{\text{ex}}^b$	$k_{\text{H}}/\text{M}^{-1}\text{ s}^{-1}$	$k_{\text{rel}}^c$
DMF	isooctane	266	$7.7 \pm 0.1 \times 10^6$	7.9
	benzene	355	$3.1 \pm 0.1 \times 10^6$	3.2
	MBOH	355	$1.38 \pm 0.03 \times 10^6$	1.4
	MeCN <sup>d</sup>	266	$1.24 \pm 0.02 \times 10^6$	1.3
	MeCN	355	$1.32 \pm 0.02 \times 10^6$	1.35
	MeOH	355	$9.8 \pm 0.2 \times 10^5$	1.0
FPRD	TFE	266	$< 1 \times 10^4$	<0.01
	isooctane	266	$3.31 \pm 0.03 \times 10^7$	12.2
	benzene	355	$1.08 \pm 0.02 \times 10^7$	4.0
	MBOH	355	$6.9 \pm 0.2 \times 10^6$	2.5
	MeCN <sup>e</sup>	266	$4.93 \pm 0.02 \times 10^6$	1.8
	MeOH	355	$2.72 \pm 0.01 \times 10^6$	1.0
DMA	isooctane	266	$5.4 \pm 0.1 \times 10^6$	4.8
	benzene	355	$2.6 \pm 0.2 \times 10^6$	2.3
	MBOH	355	$1.73 \pm 0.02 \times 10^6$	1.5
	MeCN <sup>d</sup>	266	$1.24 \pm 0.03 \times 10^6$	1.1
	MeOH	355	$1.13 \pm 0.03 \times 10^6$	1.0
	TFE	266	$< 1 \times 10^4$	<0.01
APRD	isooctane	266	$3.9 \pm 0.1 \times 10^7$	6.4
	benzene	355	$1.60 \pm 0.02 \times 10^7$	2.6
	MBOH	355	$1.19 \pm 0.03 \times 10^7$	2.0
	MeCN <sup>e</sup>	266	$9.0 \pm 0.2 \times 10^6$	1.5
	MeOH	355	$6.1 \pm 0.4 \times 10^6$	1.0
	TFE	266	$< 5 \times 10^5$	<0.08

<sup>a</sup>266 nm LFP: Ar-saturated, [dicumyl peroxide] = 0.010 M. 355 nm LFP: Ar-saturated, [dicumyl peroxide] = 0.7–1.0 M. The  $k_{\text{H}}$  values have been determined from the slope of the  $k_{\text{obs}}$  vs [substrate] plots, where the  $k_{\text{obs}}$  values have been measured following the decay of the  $\text{CumO}^\bullet$  visible absorption band. Average of at least two determinations. <sup>b</sup>Laser excitation wavelength. <sup>c</sup>As compared to MeOH. <sup>d</sup>Reference 16. <sup>e</sup>Reference 21.

**Table 2.** Second-Order Rate Constants for Reaction of the Cumyloxy Radical ( $\text{CumO}^\bullet$ ) with DMF, DMF-*d*<sub>1</sub>, DMF-*d*<sub>6</sub>, and DMF-*d*<sub>7</sub>, Measured in Acetonitrile and Isooctane at  $T = 25\text{ }^\circ\text{C}$ <sup>a</sup>

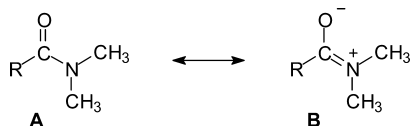
	$k_{\text{H}}/\text{M}^{-1}\text{ s}^{-1}$	
	acetonitrile <sup>b</sup>	isooctane
DMF	$1.24 \pm 0.02 \times 10^6$	$7.7 \pm 0.1 \times 10^6$
DMF- <i>d</i> <sub>1</sub>	$6.90 \pm 0.06 \times 10^5$	$4.8 \pm 0.2 \times 10^6$
$k_{\text{H}}/k_{\text{D}}$	1.8	1.6
DMF- <i>d</i> <sub>6</sub>	$7.47 \pm 0.05 \times 10^5$	$8.11 \pm 0.05 \times 10^6$
$k_{\text{H}}/k_{\text{D}}$	1.7	0.95
DMF- <i>d</i> <sub>7</sub>	$2.4 \pm 0.1 \times 10^5$	$4.2 \pm 0.1 \times 10^6$
$k_{\text{H}}/k_{\text{D}}$	5.2	1.8

<sup>a</sup>266 nm LFP: Ar-saturated, [dicumyl peroxide] = 0.010 M. The  $k_{\text{H}}$  values have been obtained from the slope of the  $k_{\text{obs}}$  vs [substrate] plots, where the  $k_{\text{obs}}$  values have been measured following the decay of the  $\text{CumO}^\bullet$  visible absorption band. Average of at least two determinations. <sup>b</sup>Reference 16.

knowledge, these represent by far the largest KSEs observed for HAT from C–H bonds to alkoxy radicals.

Amides are characterized by a pronounced C(O)–N double bond character exemplified, for a generic *N,N*-dimethylalkaneamide, by the contribution of the dipolar structure **B** to the resonance hybrid (Scheme 2). It is well established that the relative importance of structure **B** increases with increasing

Scheme 2



solvent polarity, leading to a decrease in C=O bond order and to a corresponding increase in C(O)–N bond order. Evidence in this respect has been provided by IR and NMR studies that have clearly shown that with DMF and DMA, as well as with other amides, an increase in solvent polarity leads to a decrease in the frequency of the stretching vibration of the amide I band ( $\nu(\text{C}=\text{O})$ ),<sup>22,23</sup> a decrease in the <sup>17</sup>O NMR chemical shift,<sup>22</sup> an increase in the <sup>13</sup>C NMR chemical shift,<sup>23</sup> and an increase in the activation free energy for rotation around the C(O)–N bond.<sup>24</sup> This behavior has been explained on the basis of solvent–amide dipole–dipole interactions and of solvent hydrogen bonding to the amide oxygen atom, with the largest effects that have been observed in strong HBD solvents such as water and fluorinated alcohols.

By increasing the extent of positive charge at nitrogen, polar solvents will increase the electron deficiency of the C–H bonds that are  $\alpha$  to nitrogen in DMF, FPRD, DMA, and APRD, deactivating these bonds toward HAT to an electrophilic radical such as CumO<sup>•</sup>,<sup>12a</sup> thus providing a rationale for the observed KSEs. On the basis of this picture, deactivation is also expected for the formyl C–H bond of DMF and FPRD. As mentioned above, the transition state for HAT from C–H bonds to oxygen-centered radicals is characterized by the development of positive charge on the incipient carbon-centered radical and accordingly, as compared to apolar solvents, the increase in the extent of charge separation in the amides determined by polar solvents will lead to a destabilization of the transition state. This explanation is in full agreement with previous studies that have shown that the  $k_{\text{H}}$  value for HAT from the formyl C–H bond of compounds HCOX to *t*BuO<sup>•</sup> decreases in the order aldehyde (X = alkyl, aryl) > amide (X = N(CH<sub>3</sub>)<sub>2</sub>) > ester (X = OCH<sub>2</sub>CH<sub>3</sub>), i.e. with increasing the electron withdrawing character of the X group.<sup>25,26</sup>

Interestingly, the KSEs obtained for the four amides follow a trend that is very similar to that observed previously for the reactions of CumO<sup>•</sup> with propanal and 2,2-dimethylpropanal,<sup>10</sup> with the  $k_{\text{H}}$  values that decrease in the order isooctane > benzene > MBOH > MeCN > MeOH, but different from the trend observed for the reactions of CumO<sup>•</sup> with triethylamine,<sup>11</sup> where  $k_{\text{H}}$  decreases in the order isooctane ~ benzene > MeCN > *t*BuOH > MeOH. The 2- to 3-fold decrease in  $k_{\text{H}}$  measured on going from isooctane to benzene can be explained on the basis of the formation of  $\pi$ -complexes between benzene and the amide group,<sup>27</sup> an interaction that is also possible for aldehydes but not for tertiary amines where, accordingly, comparable reactivities have been measured in these two solvents. The inversion in the  $k_{\text{H}}$  values for tertiary alcohols and MeCN observed on going from the amides to triethylamine reasonably reflects the operation of steric effects<sup>8c</sup> that limit the

accessibility of the hindered alcohol to an sp<sup>2</sup> HBA center (the amide oxygen) as compared to an sp<sup>3</sup> one (the amine nitrogen).<sup>28</sup>

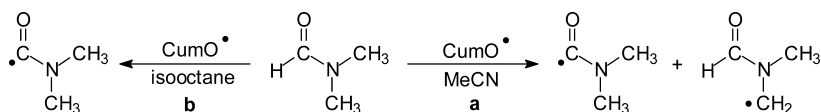
The effect of TFE on  $k_{\text{H}}$  is instead significantly more pronounced for the amides than for the aldehydes. An almost 2-fold decrease in  $k_{\text{H}}$  was measured for the reactions of CumO<sup>•</sup> with propanal and 2,2-dimethylpropanal on going from MeOH to TFE,<sup>10</sup> a >100-fold decrease in  $k_{\text{H}}$  was measured for the corresponding reactions of DMF and DMA, and a >12-fold decrease in  $k_{\text{H}}$  for those involving APRD. TFE is a stronger HBD solvent than MeOH (as measured by Abraham's  $\alpha_2^{\text{H}}$  parameters: 0.567 and 0.367, respectively),<sup>29</sup> and amides are characterized by HBA abilities significantly higher than those of aldehydes (as measured by Abraham's  $\beta_2^{\text{H}}$  parameters: 0.66, 0.73 and 0.39, respectively, for DMF, DMA, and propanal).<sup>14</sup> Along this line, a significantly stronger hydrogen bonding will result from the interaction of TFE with an amide than with an aldehyde, accounting, on the basis of the mechanistic picture discussed above, for the very low HAT reactivity observed for the amides in this solvent. This result highlights the important role played by hydrogen bond interactions in HAT reactions from tertiary alkanamides, showing that these interactions can provide a very efficient method for C–H deactivation, protecting these substrates from HAT to reactive oxygen-centered radicals. In this context, it is worth mentioning that strong HBD solvents such as TFE are known to influence the conformation of peptides and proteins, a process where inter- and intramolecular hydrogen bond interactions involving the amide group play a very important role.<sup>30</sup>

The  $k_{\text{H}}$  values for reaction of CumO<sup>•</sup> with DMF, DMF-*d*<sub>1</sub>, DMF-*d*<sub>6</sub>, and DMF-*d*<sub>7</sub> in MeCN and isooctane are collected in Table 2. As previously discussed, the analysis of the  $k_{\text{H}}/k_{\text{D}}$  values measured in MeCN clearly shows that with DMF, HAT occurs from both the formyl C–H and the C–H bonds that are  $\alpha$  to nitrogen (Scheme 3, path a).<sup>16</sup>

On the other hand, when the reactions of these substrates were studied in isooctane, very similar  $k_{\text{H}}$  values were measured for DMF and DMF-*d*<sub>6</sub> and for DMF-*d*<sub>1</sub> and DMF-*d*<sub>7</sub>. Analysis of the  $k_{\text{H}}/k_{\text{D}}$  values shows that HAT from DMF-*d*<sub>6</sub> displays no significant kinetic deuterium isotope effect ( $k_{\text{H}}/k_{\text{D}} = 0.95$ ) while similar  $k_{\text{H}}/k_{\text{D}}$  values of 1.6 and 1.8 are observed for the reactions of DMF-*d*<sub>1</sub> and DMF-*d*<sub>7</sub>. These results clearly show that in isooctane solution HAT from DMF mostly occurs from the formyl C–H bond (Scheme 3, path b), indicating that changes in solvent polarity can strongly influence the reaction selectivity. Support to this mechanistic picture is also provided by pulse radiolysis studies that have shown that in aqueous solution, HAT from DMF to the hydroxyl radical exclusively occurs from the C–H bonds of the *N*-methyl groups.<sup>31</sup>

On the basis of the discussion outlined above on the KSEs observed for the reactions of CumO<sup>•</sup> with DMF and FPRD, it appears that by increasing solvent polarity and, consequently, the extent of charge separation in the amide substrate, C–H deactivation is significantly more pronounced for the formyl C–H than for the C–H bonds that are  $\alpha$  to nitrogen, an observation that is also supported by the relatively larger

Scheme 3



decreases in  $k_{\text{H}}$  measured for DMF and FPRD as compared to DMA and APRD, on going from isoctane to MeOH ( $k_{\text{H(isooc)}}/k_{\text{H(MeOH)}} = 7.9, 12.2, 4.8, \text{ and } 6.4$ , respectively, for DMF, FPRD, DMA, and APRD. See Table 1).

Taken together, the results reported in this study expand our previous findings, showing that in the reactions of amides with alkoxyl radicals the HAT reactivity can be strongly influenced by solvent effects. Very large decreases in rate constant have been measured on going from apolar solvents to strong HBD solvents such as TFE, where changes in solvent polarity can provide a method for the deactivation of amide C–H bonds toward HAT. With DMF, evidence for a solvent-dependent change in HAT selectivity has been provided, suggesting that these effects can be successfully employed as a tool to control the C–H functionalization selectivity in synthetically useful procedures based on HAT from formamides to alkoxyl radicals.

## EXPERIMENTAL SECTION

**Materials.** Spectroscopic grade 2,2,4-trimethylpentane (isooctane), benzene, 2-methyl-2-butanol (MBOH), acetonitrile, methanol, and 2,2,2-trifluoroethanol (TFE) were used in the kinetic experiments. Dicumyl peroxide, *N,N*-dimethylformamide (DMF), *N,N*-dimethylformamide-*d*<sub>1</sub> (DMF-*d*<sub>1</sub>), *N,N*-dimethylformamide-*d*<sub>6</sub> (DMF-*d*<sub>6</sub>), *N,N*-dimethylformamide-*d*<sub>7</sub> (DMF-*d*<sub>7</sub>), *N,N*-dimethylacetamide (DMA), and *N*-formylpyrrolidine (FPRD) were of the highest commercial quality available and were used as received. *N*-acetylpyrrolidine (APRD) was available from a previous study.<sup>21</sup>

**Laser Flash Photolysis (LFP) Studies.** The time-resolved kinetic studies were carried out by LFP, employing a laser kinetic spectrometer using the third harmonic or the fourth harmonic (355 or 266 nm, respectively) of a Q-switched Nd:YAG laser, delivering pulses of the duration of 8 ns. The laser energy was adjusted by the use of the appropriate filter to  $\leq 10$  mJ/pulse. A 3.5 mL quartz cell (Suprasil, 10 mm  $\times$  10 mm) was used in all the kinetic experiments. Argon-saturated solutions containing dicumyl peroxide (10 mM for the 266 nm LFP experiments, 0.7–1.0 M for the 355 nm LFP experiments) were employed. All the experiments were carried out at  $T = 25 \pm 0.5$  °C under magnetic stirring. The observed rate constants ( $k_{\text{obs}}$ ) were obtained by monitoring the decay of the cumyloxy radical (CumO $\cdot$ ) absorption band (490–520 nm) at different substrate concentrations. Substrate concentrations were obtained by direct addition, i.e. by adding increasing amounts of the pure amides to solutions of dicumyl peroxide in the different solvents employed (isooctane, benzene, 2-methyl-2-butanol, acetonitrile, methanol, and TFE). The  $k_{\text{obs}}$  values obtained from the decay traces are the average of two to five values and a reproducibility  $\leq 5\%$  was observed.

Second-order rate constants for the reactions of the cumyloxy radical with the amides (Chart 1), in the different solvents, were obtained from the slopes of the  $k_{\text{obs}}$  vs [substrate] plots. New solutions were used for every amide concentration. The correlation coefficients obtained from the linear regression were in all cases  $>0.99$ . The  $k_{\text{H}}$  values displayed in Tables 1 and 2 are obtained by averaging at least two values obtained through independent experiments, with typical errors being  $\leq 10\%$ .

## ASSOCIATED CONTENT

### Supporting Information

Experimental details. Plots of  $k_{\text{obs}}$  vs [substrate] for the reactions of CumO $\cdot$ . This material is available free of charge via the Internet at <http://pubs.acs.org>.

## AUTHOR INFORMATION

### Corresponding Author

\*E-mail: [bietti@uniroma2.it](mailto:bietti@uniroma2.it).

### Notes

The authors declare no competing financial interest.

## ACKNOWLEDGMENTS

Financial support from the Ministero dell'Istruzione dell'Università e della Ricerca (MIUR), project 2010PFLRJR (PRIN 2010-2011), is gratefully acknowledged. We thank Prof. Lorenzo Stella for the use of LFP equipment.

## REFERENCES

- (1) Ingold, K. U.; Pratt, D. A. *Chem. Rev.* **2014**, *114*, 9022–9046.
- (2) (a) Olshansky, L.; Pizano, A. A.; Wei, Y.; Stubbe, J.; Nocera, D. G. *J. Am. Chem. Soc.* **2014**, *136*, 16210–16216. (b) Duffus, B. R.; Ghose, S.; Peters, J. W.; Broderick, J. B. *J. Am. Chem. Soc.* **2014**, *136*, 13086–13089. (c) Rydzik, A. M.; Leung, I. K. H.; Kochan, G. T.; McDonough, M. A.; Claridge, T. D. W.; Schofield, C. J. *Angew. Chem., Int. Ed.* **2014**, *53*, 10925–10927. (d) Stich, T. A.; Myers, W. K.; Britt, R. D. *Acc. Chem. Res.* **2014**, *47*, 2235–2243. (e) Matthews, M. L.; Chang, W.; Layne, A. P.; Miles, L. A.; Krebs, C.; Bollinger, J. M., Jr. *Nat. Chem. Biol.* **2014**, *10*, 209–215. (f) Chang, W.; Guo, Y.; Wang, C.; Butch, S.; Rosenzweig, A. C.; Boal, A. K.; Krebs, C.; Bollinger, J. M., Jr. *Science* **2014**, *343*, 1140–1144. (g) Yosca, T. H.; Rittle, J.; Krest, C. M.; Onderko, E. L.; Silakov, A.; Calixto, J. C.; Behan, R. K.; Green, M. T. *Science* **2013**, *342*, 825–829.
- (3) (a) Maleknia, S. D.; Downard, K. M. *Chem. Soc. Rev.* **2014**, *43*, 3244–3258. (b) Yin, H.; Xu, L.; Porter, N. A. *Chem. Rev.* **2011**, *111*, 5944–5972. (c) Hawkins, C. L.; Morgan, P. E.; Davies, M. J. *Free Radic. Biol. Med.* **2009**, *46*, 965–988.
- (4) Atkinson, R.; Arey, J. *Chem. Rev.* **2003**, *103*, 4605–4638.
- (5) (a) Michaudel, Q.; Journot, G.; Regueiro-Ren, A.; Goswami, A.; Guo, Z.; Tully, T. P.; Zou, L.; Ramabhadran, R. O.; Houk, K. N.; Baran, P. S. *Angew. Chem., Int. Ed.* **2014**, *53*, 12091–12096. (b) Roiban, G.-D.; Agudo, R.; Ilie, A.; Lonsdale, R.; Reetz, M. T. *Chem. Commun.* **2014**, *50*, 14310–14313. (c) Roiban, G.-D.; Agudo, R.; Reetz, M. T. *Angew. Chem., Int. Ed.* **2014**, *53*, 8659–8663. (d) Negretti, S.; Narayan, A. R. H.; Chiou, K. C.; Kells, P. M.; Stachowski, J. L.; Hansen, D. A.; Podust, L. M.; Montgomery, J.; Sherman, D. H. *J. Am. Chem. Soc.* **2014**, *136*, 4901–4904. (e) Iwasaki, K.; Wan, K. K.; Oppedisano, A.; Crossley, S. W. M.; Shenvi, R. A. *J. Am. Chem. Soc.* **2014**, *136*, 1300–1303. (f) Canta, M.; Font, D.; Gómez, L.; Ribas, X.; Costas, M. *Adv. Synth. Catal.* **2014**, *356*, 818–830. (g) Gormisky, P. E.; White, M. C. *J. Am. Chem. Soc.* **2013**, *135*, 14052–14055.
- (6) Salamone, M.; Bietti, M. *Synlett* **2014**, *25*, 1803–1816.
- (7) Amorati, R.; Valgimigli, L. *Org. Biomol. Chem.* **2012**, *10*, 4147–4158.
- (8) (a) Litwinienko, G.; Ingold, K. U. *Acc. Chem. Res.* **2007**, *40*, 222–230. (b) Snelgrove, D. W.; Luszytyk, J.; Banks, J. T.; Mulder, P.; Ingold, K. U. *J. Am. Chem. Soc.* **2001**, *123*, 469–477. (c) Bietti, M.; Salamone, M.; DiLabio, G. A.; Jockusch, S.; Turro, N. J. *J. Org. Chem.* **2012**, *77*, 1267–1272.
- (9) Bietti, M.; Martella, R.; Salamone, M. *Org. Lett.* **2011**, *13*, 6110–6113.
- (10) Salamone, M.; Giammarioli, I.; Bietti, M. *J. Org. Chem.* **2011**, *76*, 4645–4651.
- (11) Bietti, M.; Salamone, M. *Org. Lett.* **2010**, *12*, 3654–3657.
- (12) (a) Roberts, B. P. *Chem. Soc. Rev.* **1999**, *28*, 25–35. (b) Mitroka, S.; Zimmeck, S.; Troya, D.; Tanko, J. M. *J. Am. Chem. Soc.* **2010**, *132*, 2907–2913.
- (13) The HBA ability can be quantitatively expressed by Abraham's  $\beta_2^{\text{H}}$  parameter.<sup>14</sup>  $\beta_2^{\text{H}} = 0.66\text{--}0.73$  and  $0.58\text{--}0.73$  for alkanamides and alkylamines, respectively.
- (14) Abraham, M. H.; Grellier, P. L.; Prior, D. V.; Morris, J. J.; Taylor, P. J. *J. Chem. Soc., Perkin Trans. 2* **1990**, 521–529.
- (15) See for example: (a) Tu, H.-Y.; Liu, Y.-R.; Chu, J.-J.; Hu, B.-L.; Zhang, X.-G. *J. Org. Chem.* **2014**, *79*, 9907–9912. (b) Yang, X.-H.; Wei, W.-T.; Li, H.-B.; Song, R.-J.; Li, J.-H. *Chem. Commun.* **2014**, *50*, 12867–12869. (c) Yu, H.; Shen, J. *Org. Lett.* **2014**, *16*, 3204–3207. (d) Feng, J.-B.; Wei, D.; Gong, J.-L.; Qi, X.; Wu, X.-F. *Tetrahedron Lett.* **2014**, *55*, 5082–5084. (e) Wang, R.; Liu, H.; Yue, L.; Zhang, X.-K.; Tan, Q.-Y.; Pan, R.-L. *Tetrahedron Lett.* **2014**, *55*, 2233–2237. (f) Sathish Kumar, G.; Arun Kumar, R.; Santhosh Kumar, P.; Veera

Reddy, N.; Vijaya Kumar, K.; Lakshmi Kantam, M.; Prabhakar, S.; Rajender Reddy, K. *Chem. Commun.* **2013**, *49*, 6686–6688. (g) Li, D.; Liu, J.; Zhao, Q.; Wang, L. *Chem. Commun.* **2013**, *49*, 3640–3642. (h) Wang, H.; Guo, L.-N.; Duan, X.-H. *Org. Biomol. Chem.* **2013**, *11*, 4573–4576. (i) Ding, S.; Jiao, N. *Angew. Chem., Int. Ed.* **2012**, *51*, 9226–9237.

(16) Salamone, M.; Milan, M.; DiLabio, G. A.; Bietti, M. *J. Org. Chem.* **2013**, *78*, 5909–5917.

(17) (a) Baciocchi, E.; Bietti, M.; Salamone, M.; Steenken, S. *J. Org. Chem.* **2002**, *67*, 2266–2270. (b) Avila, D. V.; Ingold, K. U.; Di Nardo, A. A.; Zerbetto, F.; Zgierski, M. Z.; Lusztyk, J. *J. Am. Chem. Soc.* **1995**, *117*, 2711–2718.

(18) Banks, J. T.; Scaiano, J. C. *J. Am. Chem. Soc.* **1993**, *115*, 6409–6413.

(19) Bietti, M.; Gente, G.; Salamone, M. *J. Org. Chem.* **2005**, *70*, 6820–6826.

(20) Avila, D. V.; Brown, C. E.; Ingold, K. U.; Lusztyk, J. *J. Am. Chem. Soc.* **1993**, *115*, 466–470.

(21) Salamone, M.; Milan, M.; DiLabio, G. A.; Bietti, M. *J. Org. Chem.* **2014**, *79*, 7179–7184.

(22) Gerathanassis, I. P.; Vakka, C. *J. Org. Chem.* **1994**, *59*, 2341–2348.

(23) Eaton, G.; Symons, M. C. R. *J. Chem. Soc., Faraday Trans. 1* **1988**, *84*, 3459–3473.

(24) Wiberg, K. B.; Rablen, P. R.; Rush, D. J.; Keith, T. A. *J. Am. Chem. Soc.* **1995**, *117*, 4261–4270.

(25) Chatgililoglu, C.; Lunazzi, L.; Macciantelli, D.; Placucci, G. *J. Am. Chem. Soc.* **1984**, *106*, 5252–5256.

(26) As compared to the present study where the effect of different solvents on the reactivity of a given amide substrate has been considered, in the study described in ref 25 the same solvent system (benzene:di-*tert*-butyl peroxide 1:2 (v/v)) was used for the reactions of all substrates with *t*BuO<sup>•</sup>. Along this line, the observation that under these conditions the formyl C–H bond of ethyl formate (X = OEt) is significantly less reactive than the formyl C–H bond of DMF (X = NMe<sub>2</sub>) clearly indicates that, as compared to the latter substrate, in the former substrate the relative contribution to C–H deactivation determined by the electron-withdrawing character of the X group is significantly more important than the contribution deriving from internal charge separation.

(27) (a) Stewart, W. E.; Siddall, T. H., III. *Chem. Rev.* **1970**, *70*, 517–551. (b) Moriarty, R. M. *J. Org. Chem.* **1963**, *28*, 1296–1299.

(28) As pointed out by a reviewer, this hypothesis seems to contradict the similar HBA abilities observed for alkanamides and alkylamines.<sup>13,14</sup> It is however important to point out that the available  $\beta_2^H$  values for these substrates have been generally obtained by employing unhindered reference acids in carbon tetrachloride, where, most importantly, the sterically hindered reference acid 2-methyl-2-propanol was observed to display a significantly different behavior as compared to primary alkanols.<sup>14</sup>

(29) Abraham, M. H.; Grellier, P. L.; Prior, D. V.; Duce, P. P.; Morris, J. J.; Taylor, P. J. *J. Chem. Soc., Perkin Trans. 2* **1989**, 699–711.

(30) See for example: (a) Xiong, K.; Asher, S. A. *Biochemistry* **2010**, *49*, 3336–3342. (b) Starzyk, A.; Barber-Armstrong, W.; Sridharan, M.; Decatur, S. M. *Biochemistry* **2005**, *44*, 369–376. (c) Walgers, R.; Lee, T. C.; Cammers-Goodwin, A. *J. Am. Chem. Soc.* **1998**, *120*, 5073–5079.

(31) Hayon, E.; Ibata, T.; Lichtin, N. N.; Simic, M. *J. Am. Chem. Soc.* **1970**, *92*, 3898–3903.